Supporting Information for "Carbon outgassing in the Antarctic Circumpolar Current is supported by Ekman transport from the sea ice zone in an observation-based seasonal mixed-layer budget"

Jade Sauvé[1], Alison R. Gray[1], Channing J. Prend[1,2], Seth M. Bushinsky[3],

Stephen C. Riser[1]

[1]School of Oceanography, University of Washington, Seattle, WA, USA

[2]Environmental Science and Engineering, California Institute of Technology, Pasadena, CA, USA

[3]Department of Oceanography, School of Ocean and Earth Science and Technology, University of Hawaii at Manoa, HI, USA

Contents of this file

1. Text S1

2. Figures S1 to S17

Introduction This supporting information contains additional details for the derivation of the budget equation, as well as additional figures which may be useful for readers interested in reproducing the method.

Text S1. Derivation of Budget Equation To obtain the TEND and the F_{entrain}, we use the following equality to expand the first term of Eq. 1 (from main text).

$$\frac{\partial}{\partial t} \int_{-h(t)}^{0} \gamma dz = \int_{-h(t)}^{0} \frac{\partial(\gamma)}{\partial t} dz + \frac{dh}{dt} \gamma_{-h} \tag{1}$$

———

March 8, 2023, 12:11am

:

We obtain

$$\int_A \left[\frac{\partial}{\partial t} \int_{-h(t)}^{0} \rho[X]dz - \frac{dh}{dt}(\rho[X])_{-h} \right] dA \tag{2}$$

Integrating over depth

$$\int_A \left[\frac{\partial(\rho[X](0+h))}{\partial t} - \frac{dh}{dt}(\rho[X])_{-h} \right] dA \tag{3}$$

Simplifying and integrating over the area

$$A\frac{\partial(\rho[X]h)}{\partial t} - A(\rho[X])_{-h}\frac{dh}{dt} \tag{4}$$

where

$$F_{entrain} = \rho_{-h}[X]_{-h}\frac{dh}{dt} \quad if \quad \frac{dh}{dt} > 0 \tag{5}$$

$$F_{entrain} = \rho[X]\frac{dh}{dt} \quad if \quad \frac{dh}{dt} < 0 \tag{6}$$

The advective flux terms originate from the second term of Eq. 1 (from main text). We separate the horizontal and vertical advections by expanding the dot product.

$$\int_A \int_{-h(t)}^{0} \left(u\frac{\partial(\rho[X])}{\partial x} + v\frac{\partial(\rho[X])}{\partial y} \right) dzdA + \int_A \int_{-h(t)}^{0} w\partial(\rho[X])dA \tag{7}$$

where (u,v,w) is the velocity vector in the (x,y,z) direction. We can ignore the zonal advection term (v) due to the shape of the zone which is approximately zonally symmetric. We assume that the meridional gradient of the molar concentration of tracer ($\rho[X]$) doesn't vary with depth in the mixed layer.

$$\int_A \frac{\partial(\rho[X])}{\partial y} \int_{-h(t)}^{0} vdzdA + \int_A w\rho[X]|_{-h(t)}^{0}dA \tag{8}$$

In the Southern Ocean, meridional advection at the surface is mostly due to Ekman transport with additional contribution from geostrophic transport. We assume that the

Ekman depth is smaller than the mixed layer depth.

$$\int_A \frac{\partial(\rho[X])}{\partial y} \int_{-h(t)}^{0} (v_{ek} + v_{geo})dzdA + \int_A \left[w\rho[X]|_0 - w\rho[X]|_{-h} \right] dA \tag{9}$$

Since vertical velocity (w) is 0 at the surface and using the following Coriolis equation,

$$\int_{-h(t)}^{0} \rho v_{ek} dz = -\frac{\tau_x}{f} \tag{10}$$

we obtain the following equation, having further assumed that the meridional gradient of the molar concentration of tracer ($\rho[X]$) doesn't vary zonally.

$$\int_y \frac{\partial(\rho[X])}{\partial y} \int_x \left[\frac{-\tau_x}{f\rho} + \int_{-h(t)}^{0} v_{geo}dz \right] dxdy - A(w\rho[X])|_{-h} \tag{11}$$

We simplify further and set the boundaries of the meridional integration as the Northern (N) and Southern (S) frontal boundaries.

$$\int_S^N \partial(\rho[X]) \int_x \left[\frac{-\tau_x}{f\rho} + \int_{-h(t)}^{0} v_{geo}dz \right] dx - A(w\rho[X])|_{-h} \tag{12}$$

We define V_{ek} and V_{geo}, the Ekman and geostrophic mass transports,

$$\int_S^N V_{ek}\partial(\rho[X]) + \int_S^N V_{geo}\partial(\rho[X]) - A(w\rho[X])|_{-h} \tag{13}$$

and divide through by the ocean surface area to obtain the final form of the horizontal advection equation, as consistent with Eq. 3 (from main text).

$$F_{horiz-adv} = -\frac{1}{A} \left[(\rho[X]V_{ek})|_N - (\rho[X]V_{ek})|_S + (\rho[X]V_{geo})|_N - (\rho[X]V_{geo})|_S \right] \tag{14}$$

$\rho[X]|_N$ ($\rho[X]|_S$) corresponds to the tracer molar concentration of the source water of the horizontal advection at the northern (southern) boundary.

The vertical advection at the base of the mixed layer depends on the vertical velocity at the base of the mixed layer (w_{-h}) as well as on the molar concentration of tracer ($\rho[X]|_{-h}$) in the downwelled or upwelled waters depending on the sign of w_{-h}.

March 8, 2023, 12:11am

:

$$F_{vert-adv} = (w\rho[X])|_{-h} \tag{15}$$

The mixing flux term corresponds to the last term of Eq. 1 (from main text), which can be expressed as

$$\int_A \kappa_z \frac{\partial(\rho[X])}{\partial z}\Big|_{-h}^{0} dA \tag{16}$$

Since the vertical gradient of the molar concentration is 0 at the surface and integrating over the ocean surface area, we are left with

$$-A\kappa_z \frac{\partial(\rho[X])}{\partial z}\Big|_{-h} \tag{17}$$

Dividing by the area for consistency with Eq. 3 (from main text), we obtain

$$F_{mixing} = -\kappa_z \frac{\partial(\rho[X])}{\partial z}\Big|_{-h} \tag{18}$$

References

March 8, 2023, 12:11am
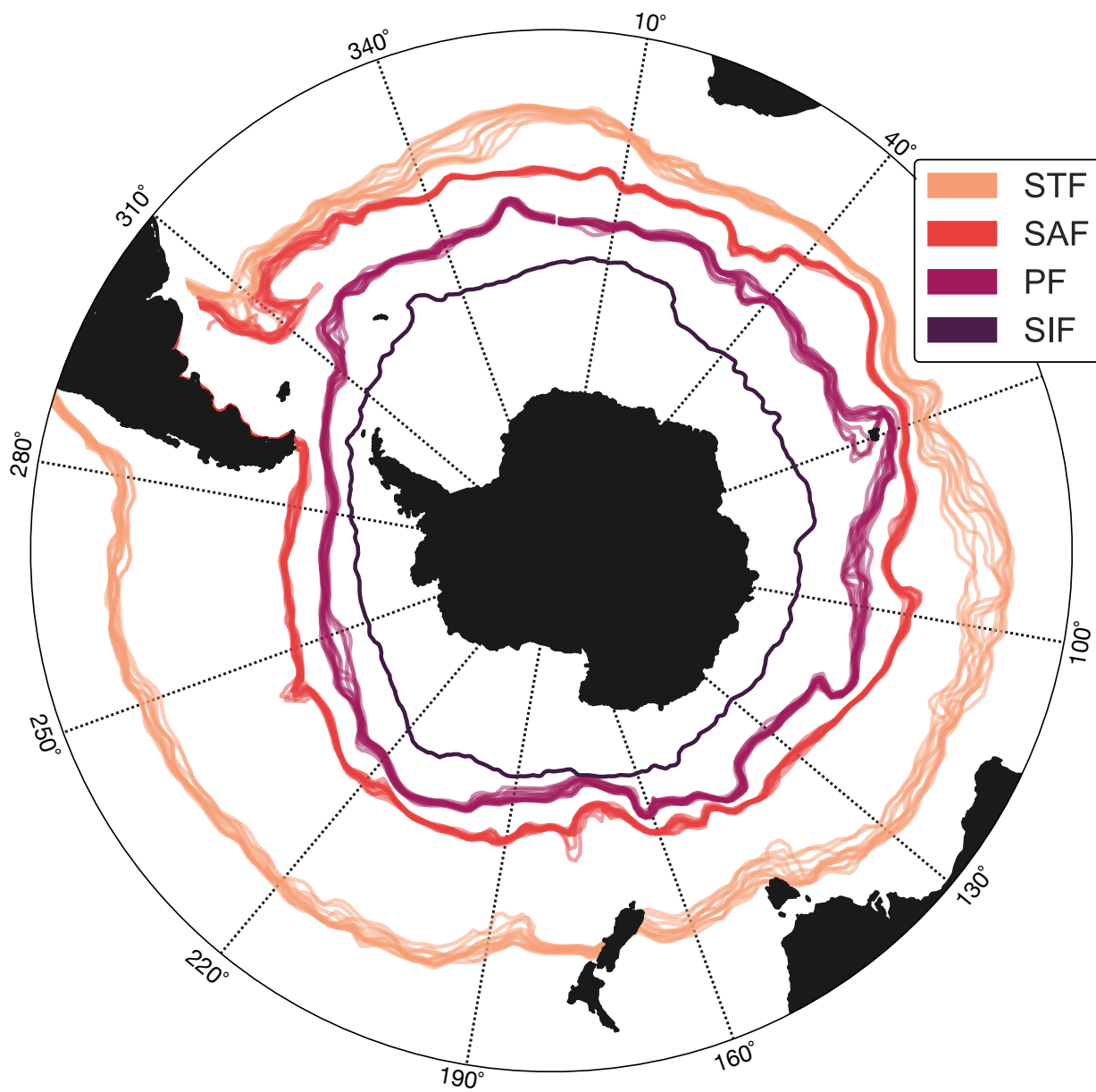
Figure S1. Monthly position of the fronts used to define the frontal regions. (STF: Subtropical Front, SAF: Sub-Antarctic Front, PF: Polar Front, SIF: Sea Ice Front).

March 8, 2023, 12:11am

:
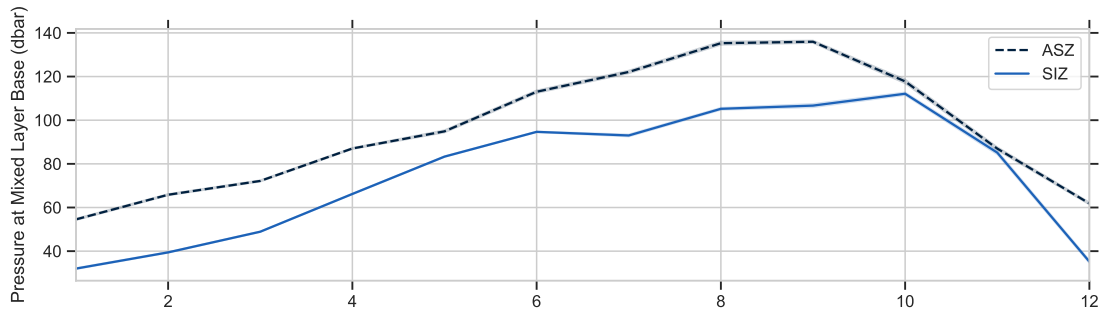
Figure S2. Monthly pressure at the base of the mixed layer for the ASZ and the SIZ.
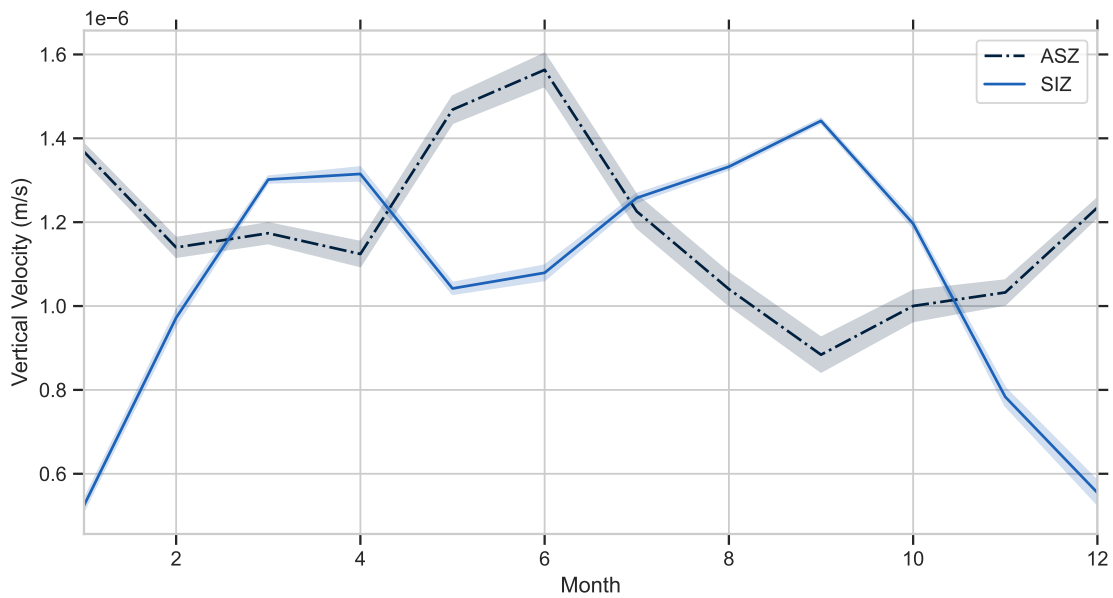
Figure S3. Vertical Velocity at the base of the mixed layer estimated using the mixed layer mass budget

March 8, 2023, 12:11am
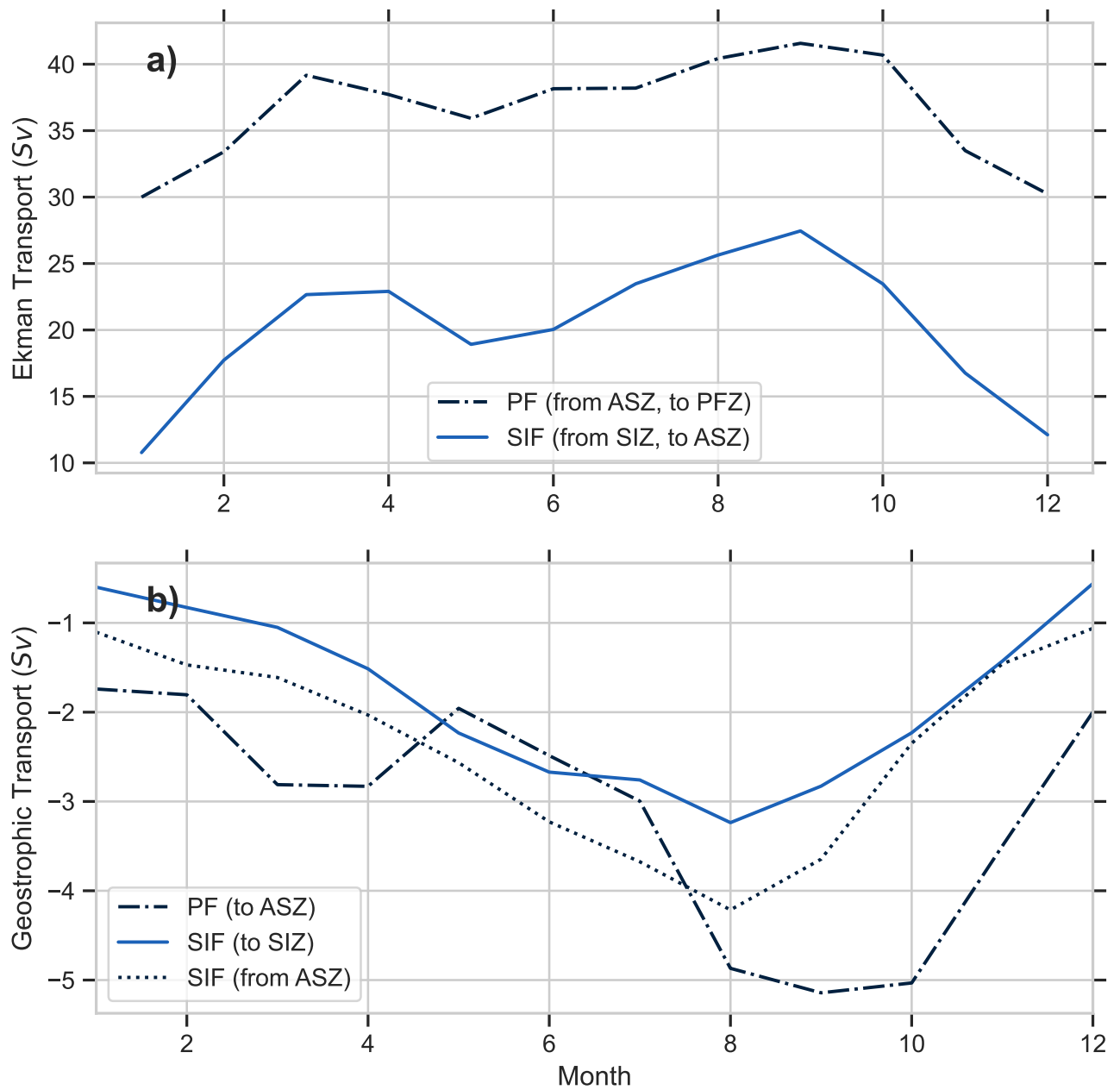
Figure S4. Monthly mass transport of water due to a) Ekman and b) geostrophic transport. Geostrophic transport across a particular front varies by frontal region due to the choice of depth of integration, the mixed layer depth of the zone under consideration.

March 8, 2023, 12:11am
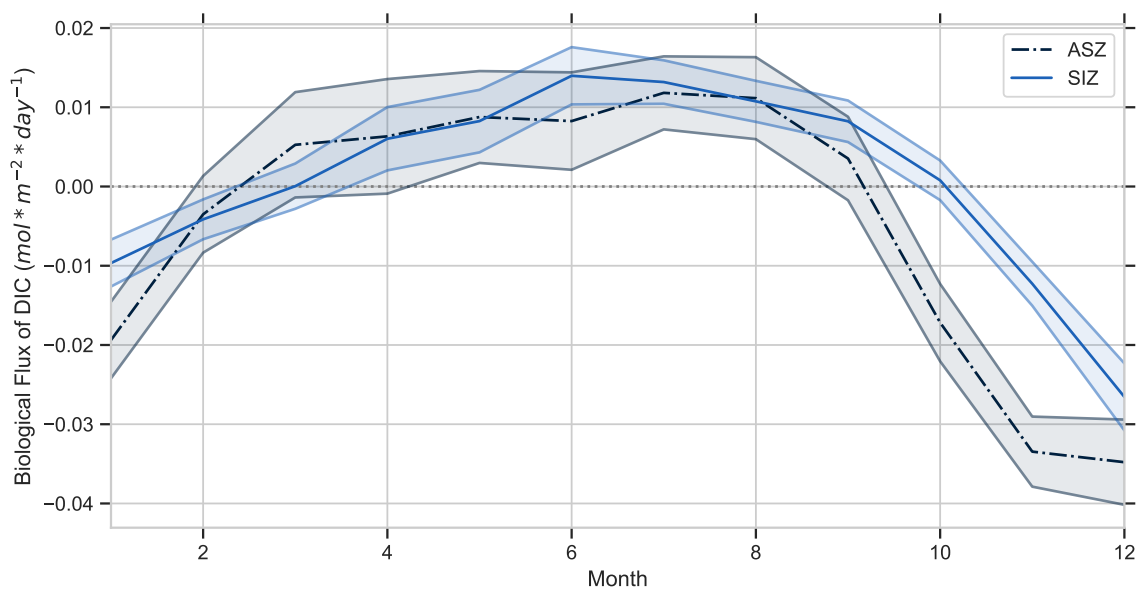
Figure S5. Monthly biological flux of carbon estimated using the optimization scheme for the ASZ and the SIZ. The shading corresponds to one standard deviation of the Monte Carlo simulation.
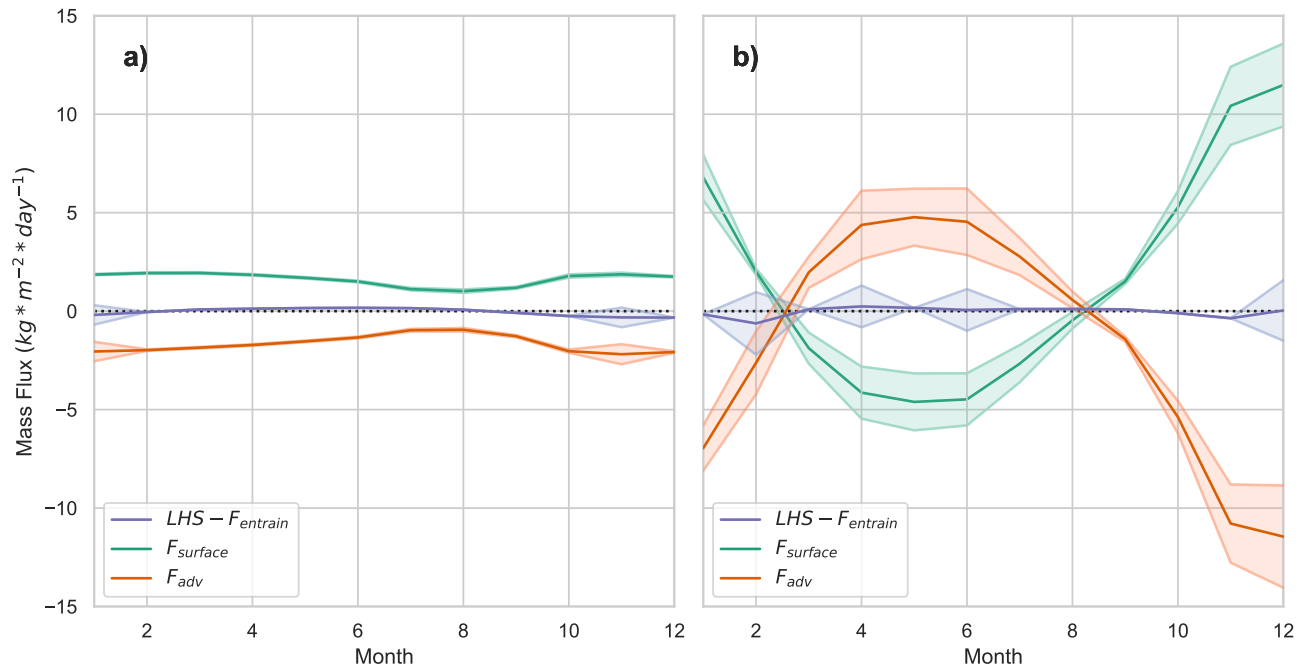
Figure S6. Monthly averaged mixed layer mass fluxes for a) the ASZ and b) the SIZ.
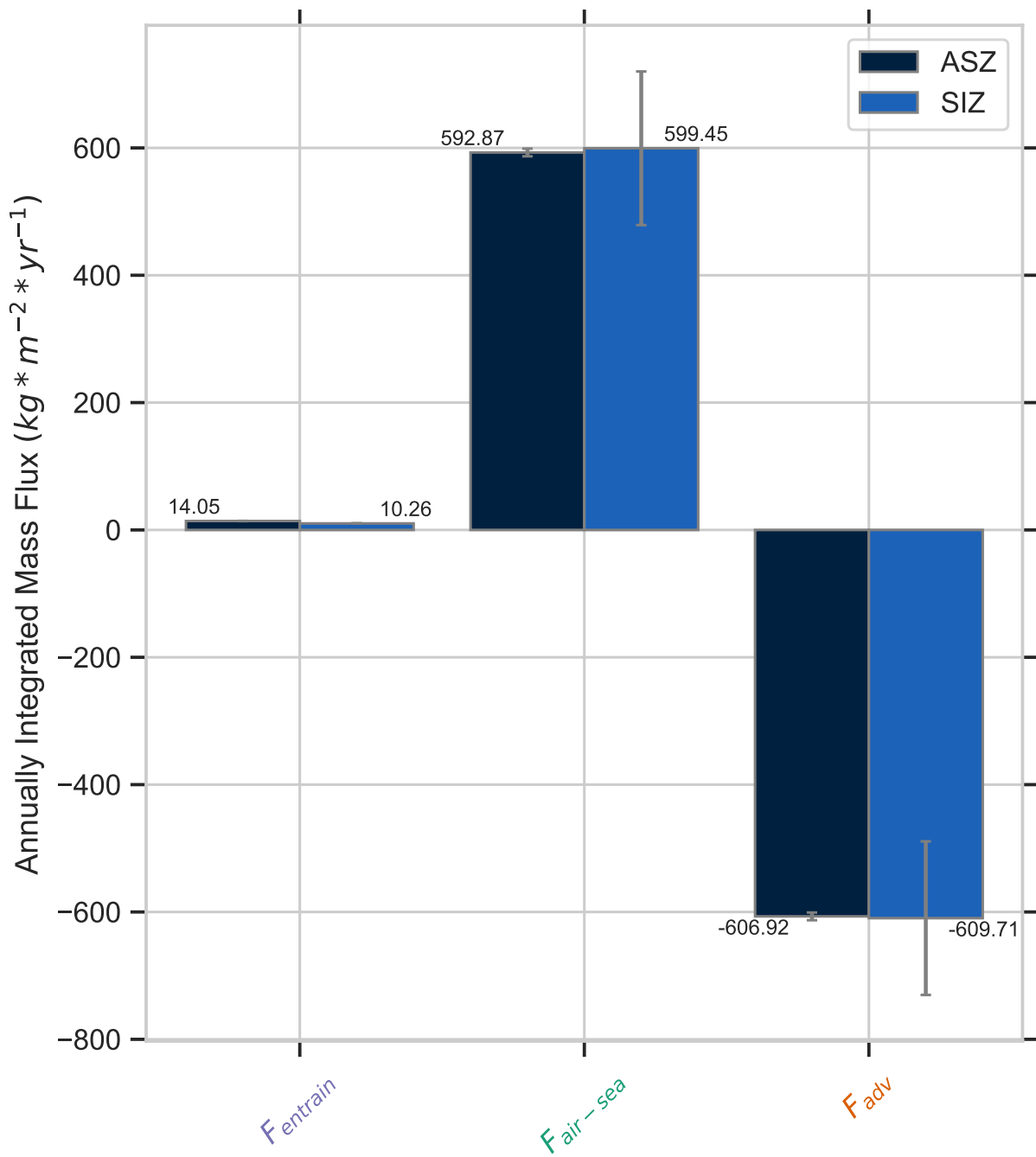
Figure S7. Annually integrated advective fluxes of mass for the ASZ and the SIZ. While this figure shows the advective fluxes of mass, advective fluxes of carbon follow the same pattern but with different magnitudes.
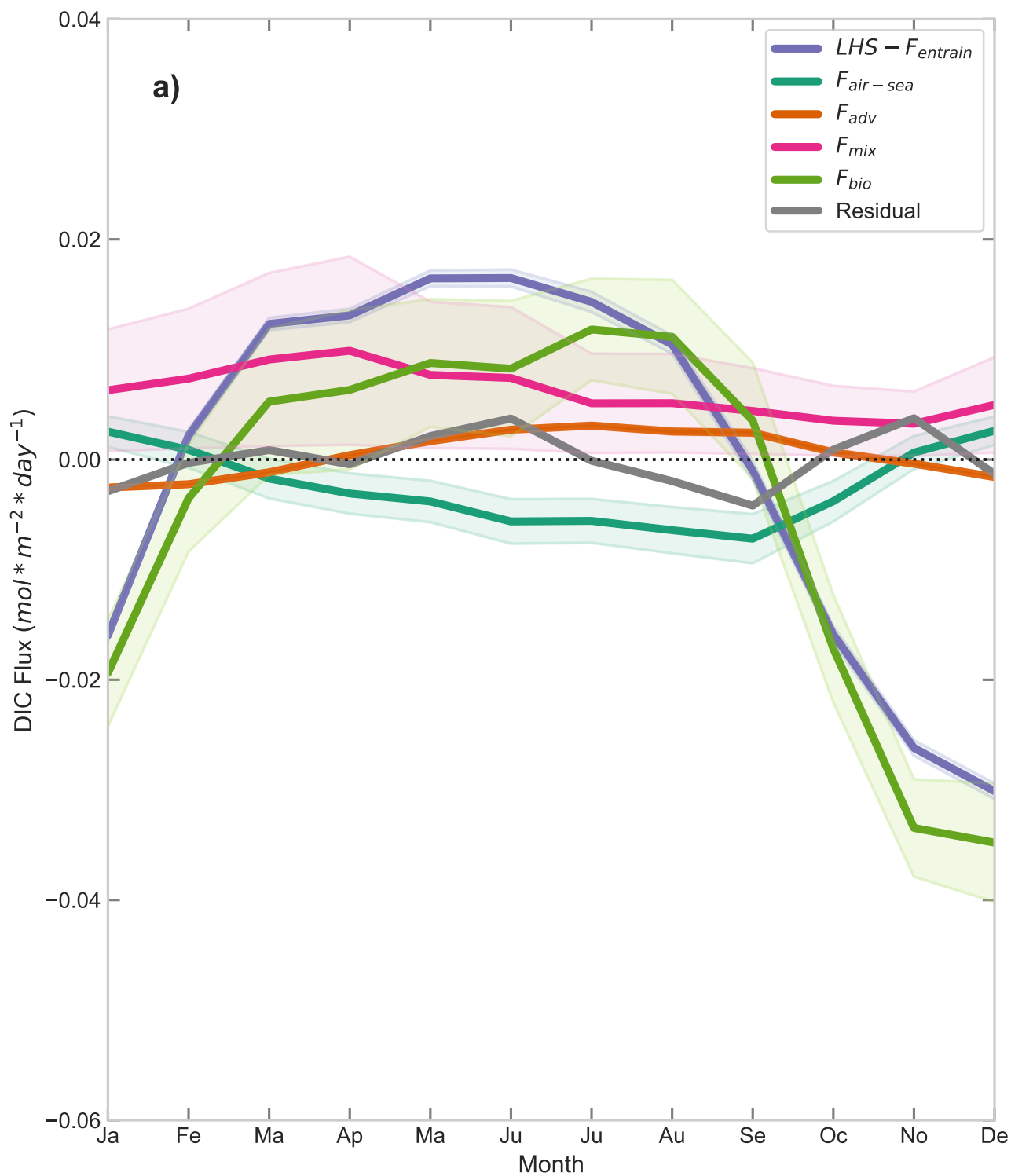
Figure S8. Monthly averaged fluxes of DIC to and from the ASZ mixed layer as well as the budget residual in gray. Fluxes are presented with an uncertainty of one standard deviation. Negative (positive) fluxes remove (add) carbon from (to) the mixed layer.

March 8, 2023, 12:11am
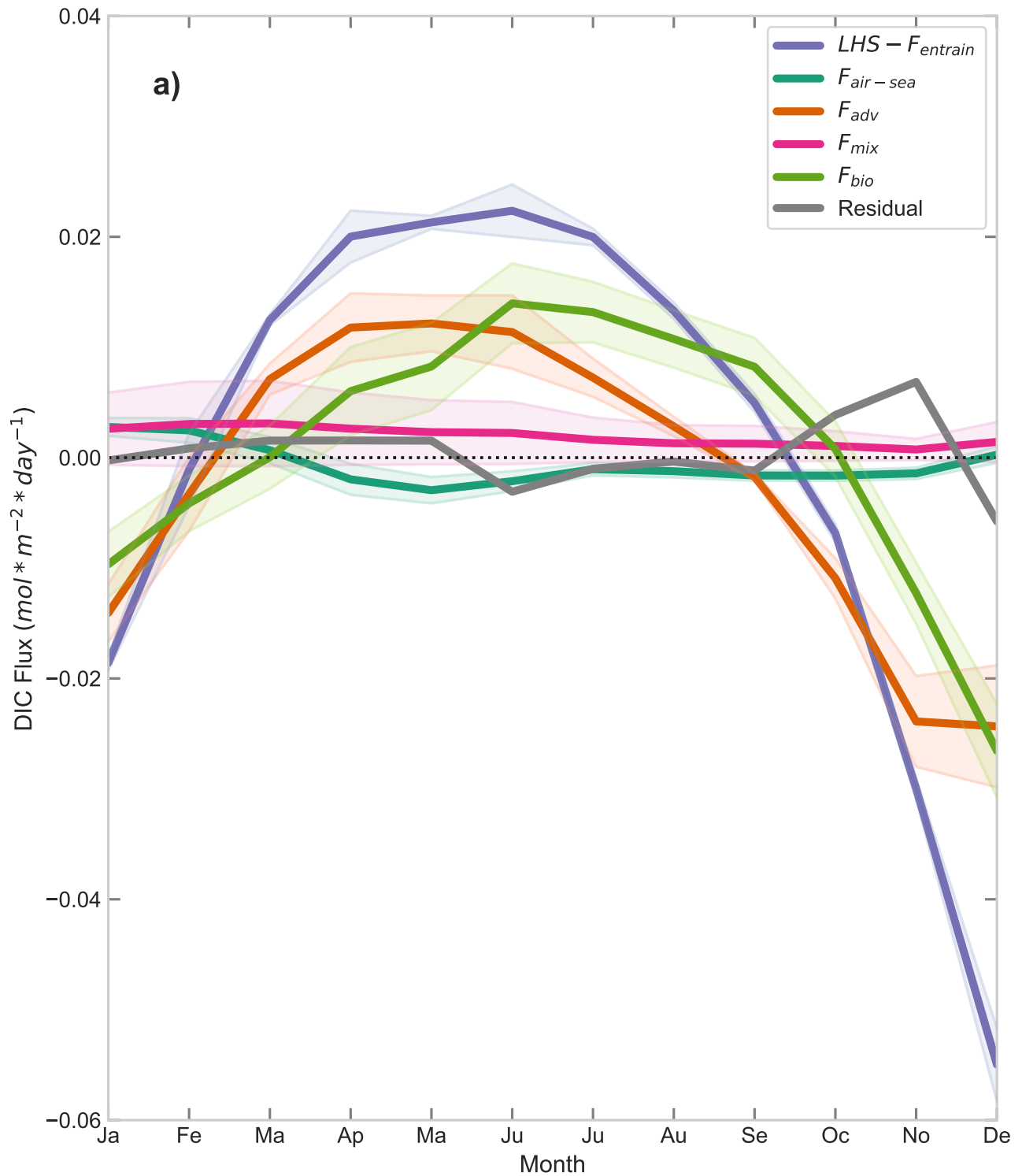
Figure S9. Monthly averaged fluxes of DIC to and from the SIZ mixed layer as well as the budget residual in gray. Fluxes are presented with an uncertainty of one standard deviation. Negative (positive) fluxes remove (add) carbon from (to) the mixed layer.
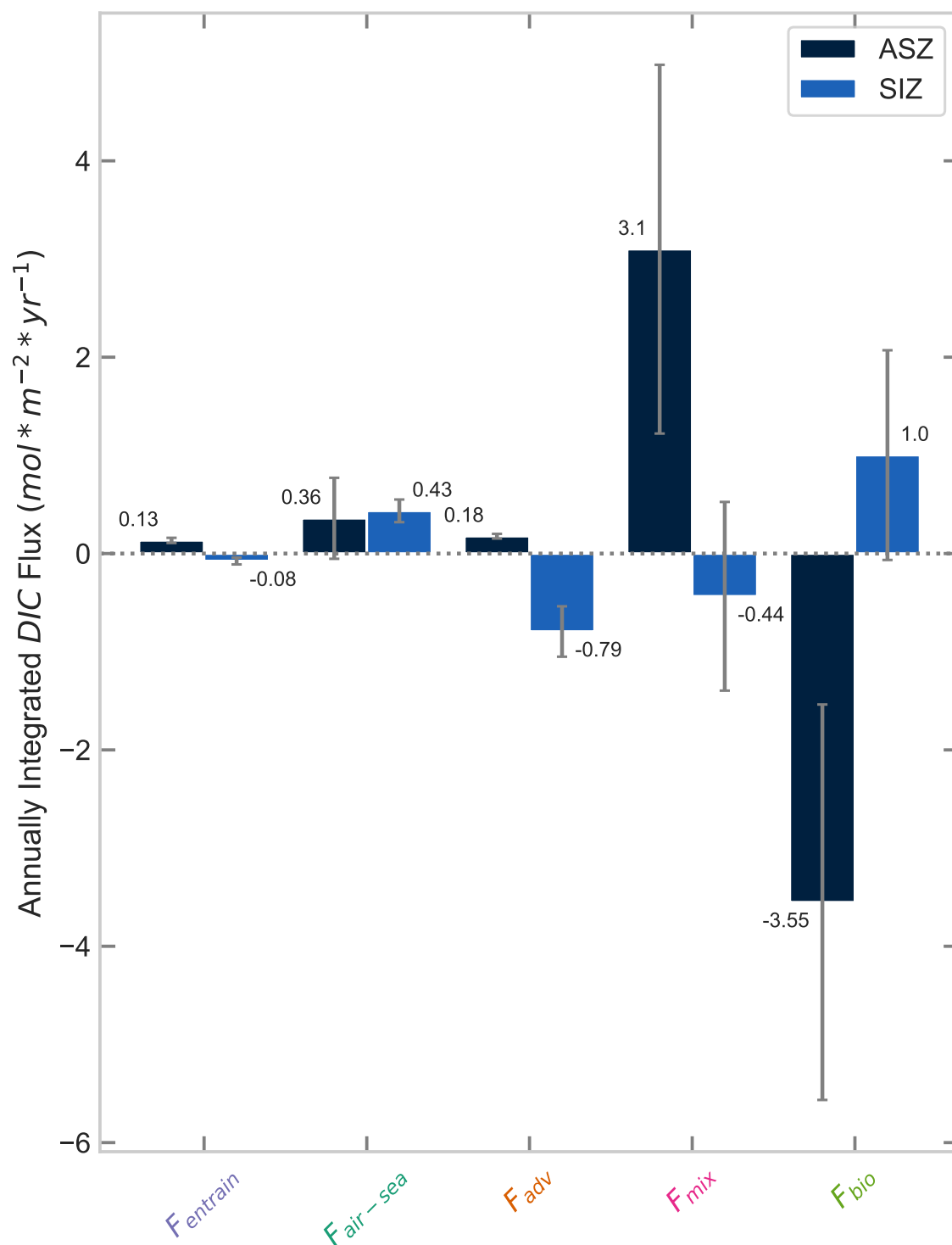
March 8, 2023, 12:11am

March 8, 2023, 12:11am

Figure S10.   Annually integrated fluxes of carbon using the SOCAT-based air-sea flux product.
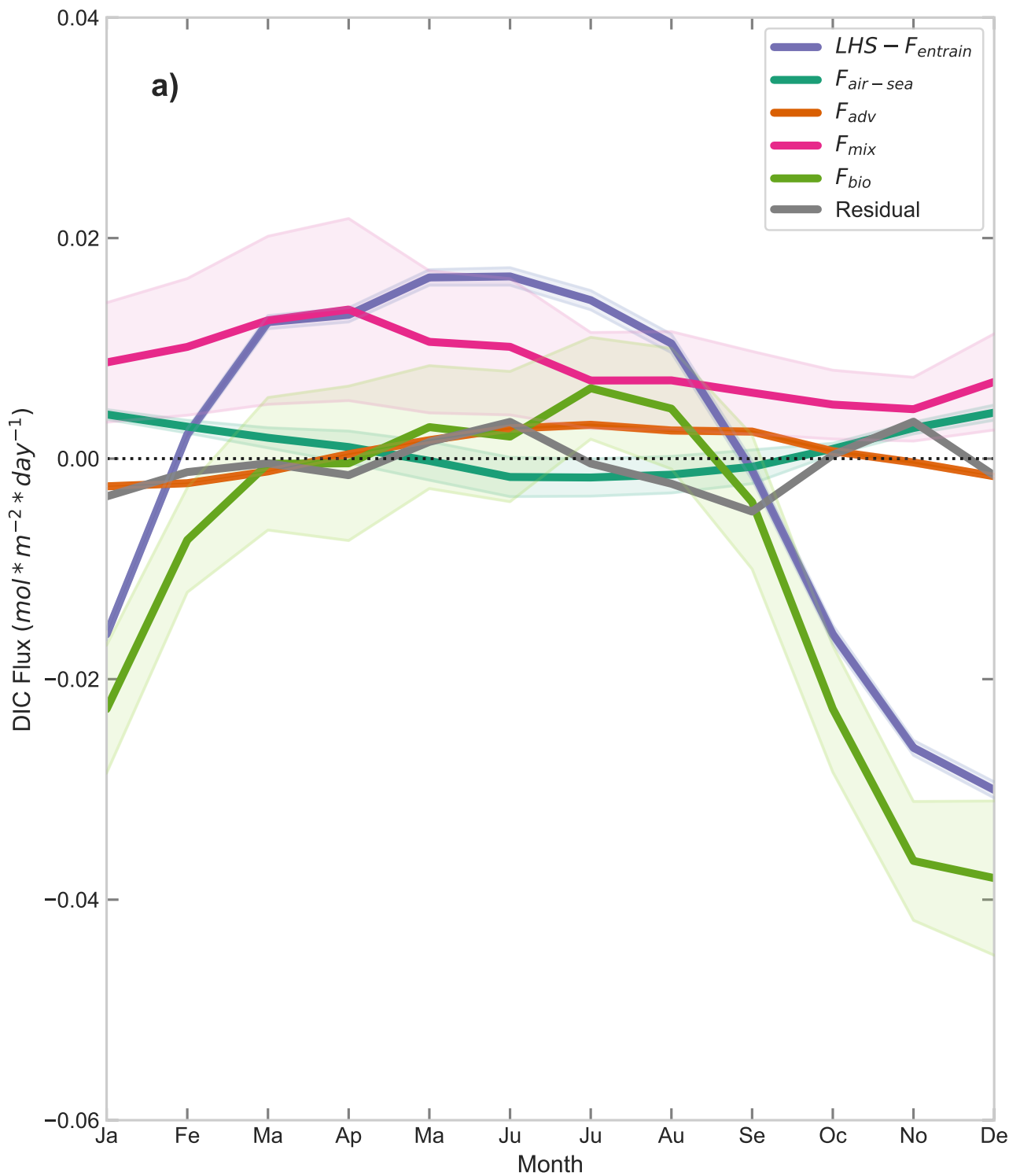
Figure S11. Monthly averaged fluxes of DIC to and from the ASZ mixed layer using the SeaFlux-based air-sea flux product. Fluxes are presented with an uncertainty of one standard deviation. Negative (positive) fluxes remove (add) carbon from (to) the mixed layer.

March 8, 2023, 12:11am
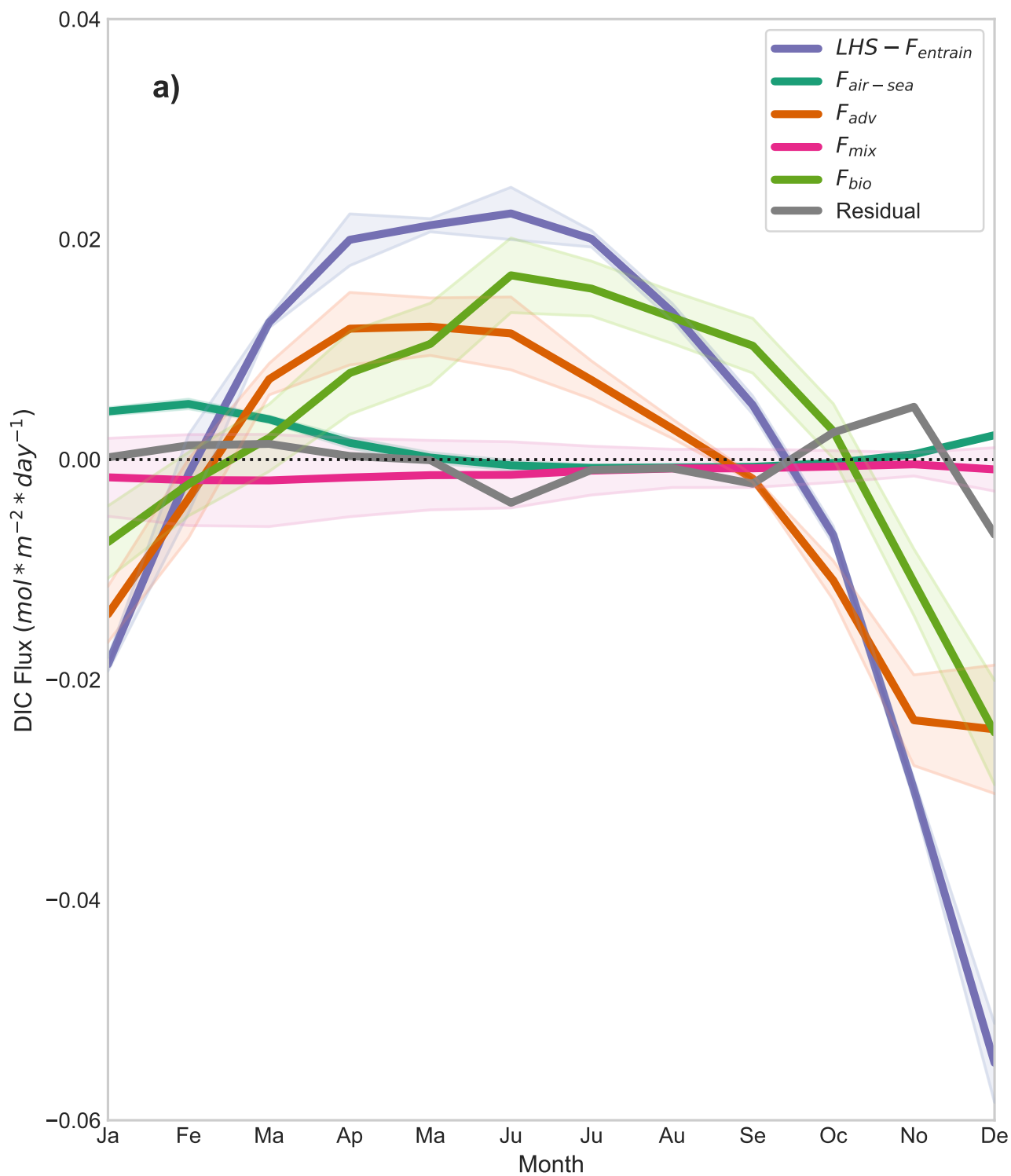
Figure S12. Monthly averaged fluxes of DIC to and from the SIZ mixed layer using the SeaFlux-based air-sea flux product. Fluxes are presented with an uncertainty of one standard deviation. Negative (positive) fluxes remove (add) carbon from (to) the mixed layer.

March 8, 2023, 12:11am
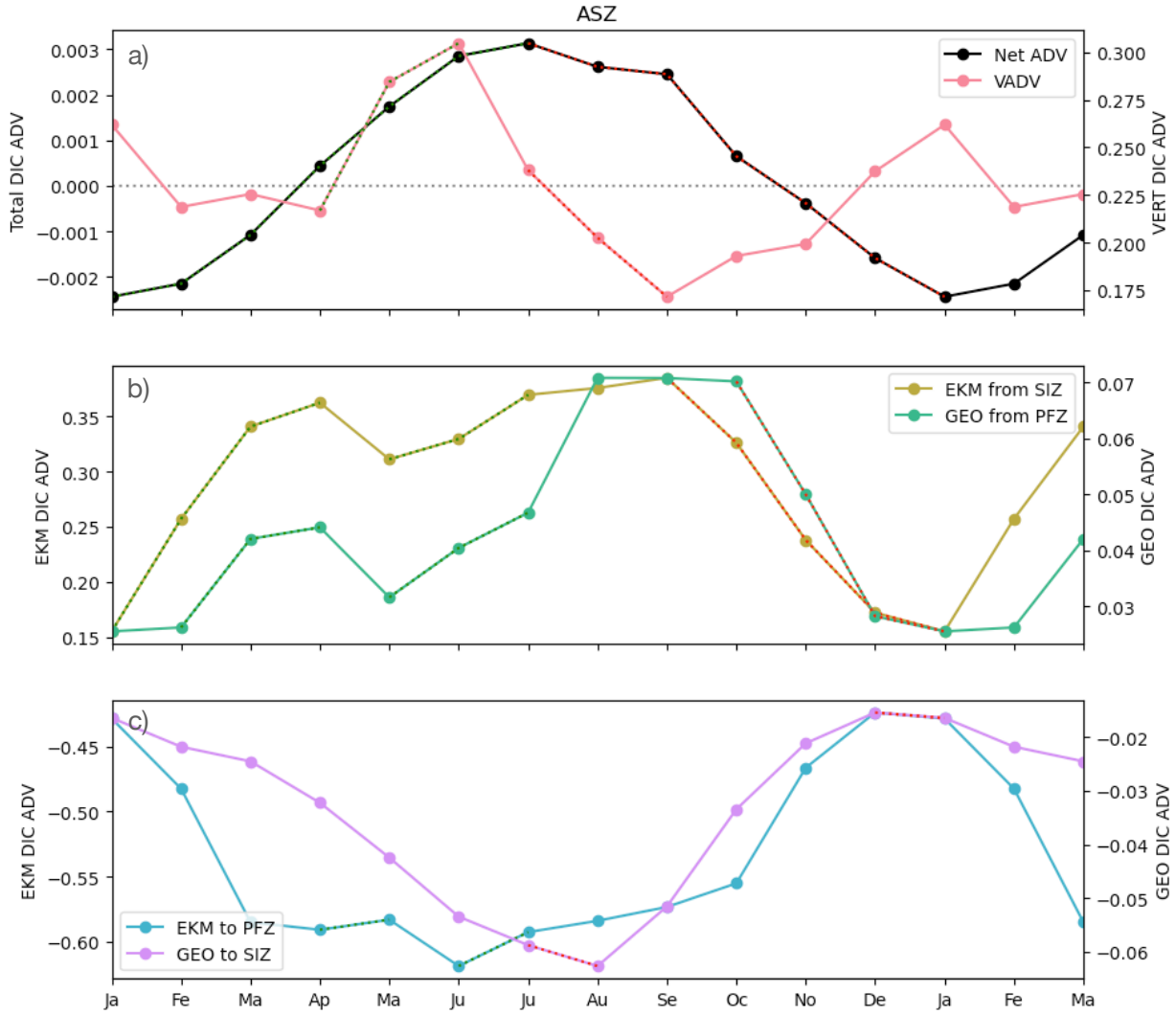
Figure S13. Monthly averaged total advective flux of DIC and its components in the ASZ (mol C *m^{-2}*day^{-1}). a) Total advective flux of DIC and vertical advective flux of DIC. b) Ekman advective flux of DIC from the SIZ and geostrophic advective flux of DIC from the PFZ. c) Ekman advective flux of DIC to the PFZ and geostrophic advective flux of DIC to the SIZ. Overlaid dotted red and green lines indicate periods where the slope of the advection component matches the sign of the slope of the total advection.
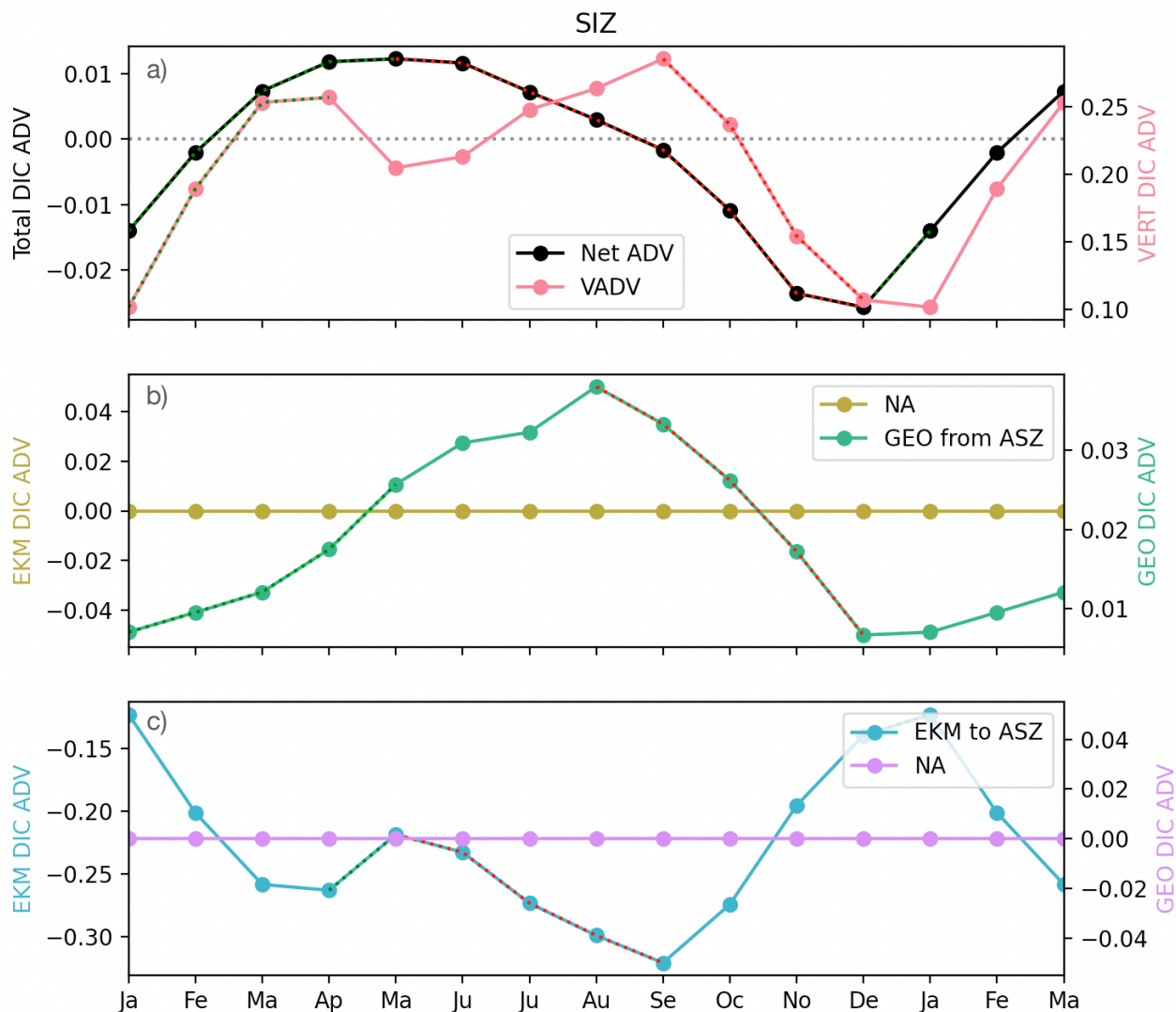
Figure S14.   Monthly averaged total advective flux of DIC and its components in the SIZ

(mol C *m^{-2}*day^{-1}). a) Total advective flux of DIC and vertical advective flux of DIC. b) Ekman

advective flux of DIC from the SIZ and geostrophic advective flux of DIC from the PFZ. c)

Ekman advective flux of DIC to the PFZ and geostrophic advective flux of DIC to the SIZ.

Overlaid dotted red and green lines indicate periods where the slope of the advection component

matches the sign of the slope of the total advection.

:
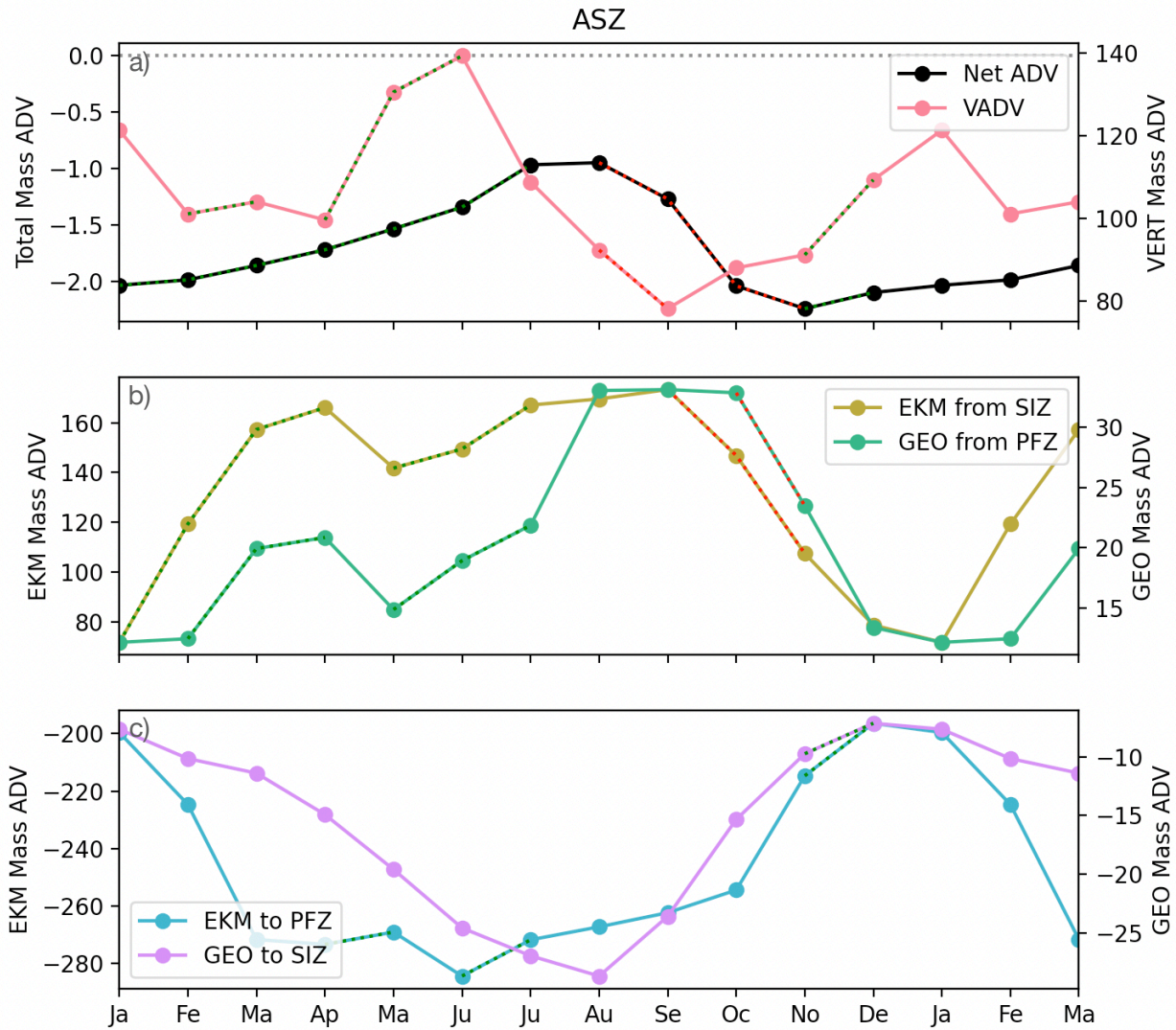
Figure S15. Monthly averaged total advective flux of mass and its components in the ASZ (kg*m^{-2}*day^{-1}). a) Total advective flux of mass and vertical advective flux of mass. b) Ekman advective flux of mass from the SIZ and geostrophic advective flux of mass from the PFZ. c) Ekman advective flux of mass to the PFZ and geostrophic advective flux of mass to the SIZ. Overlaid dotted red and green lines indicate periods where the slope of the advection component matches the sign of the slope of the total advection.
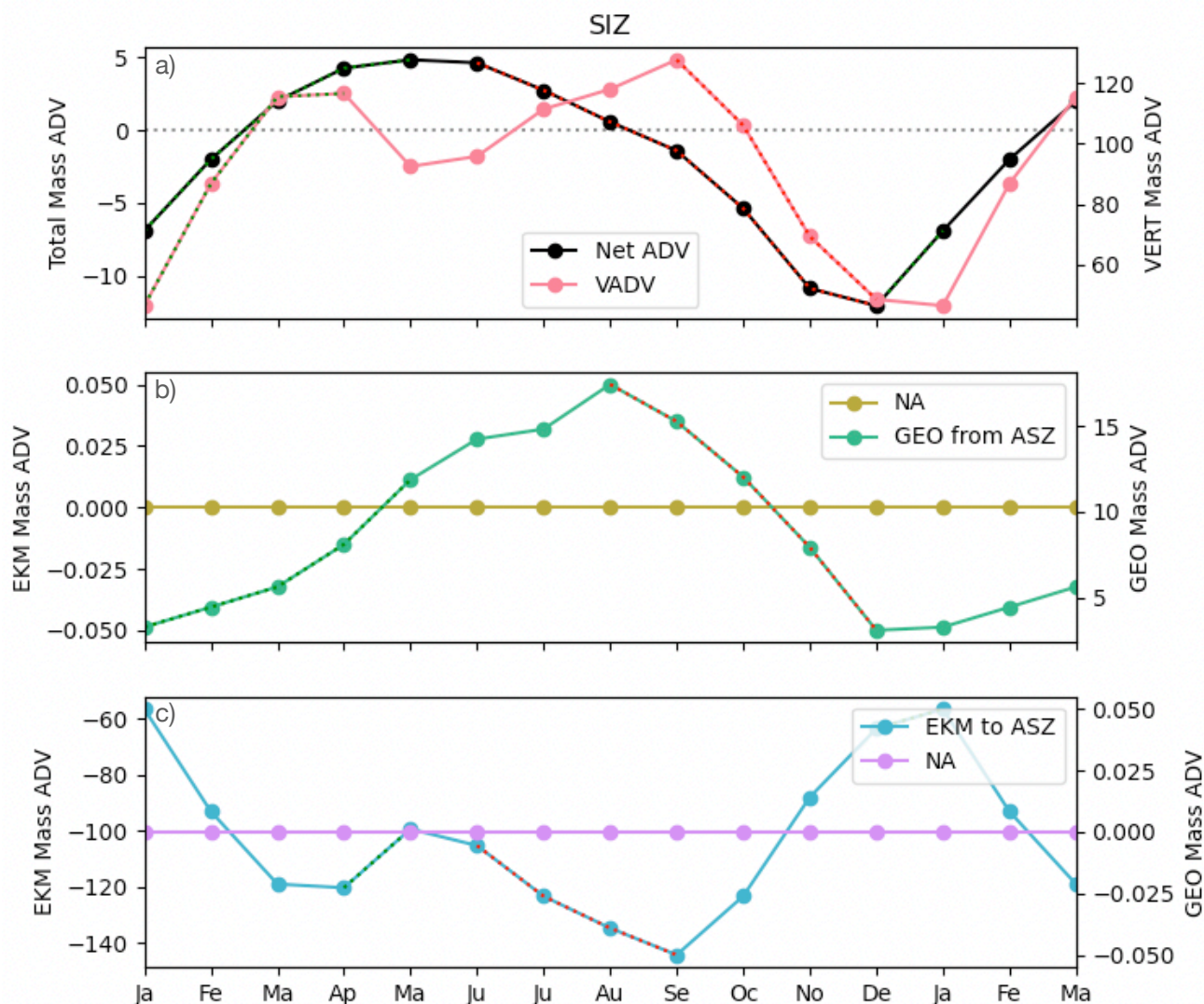
Figure S16. Monthly averaged total advective flux of mass and its components in the SIZ (kg*m^{-2}*day^{-1}). a) Total advective flux of mass and vertical advective flux of mass. b) Ekman advective flux of mass from the SIZ and geostrophic advective flux of mass from the PFZ. c) Ekman advective flux of mass to the PFZ and geostrophic advective flux of mass to the SIZ. Overlaid dotted red and green lines indicate periods where the slope of the advection component matches the sign of the slope of the total advection.

March 8, 2023, 12:11am
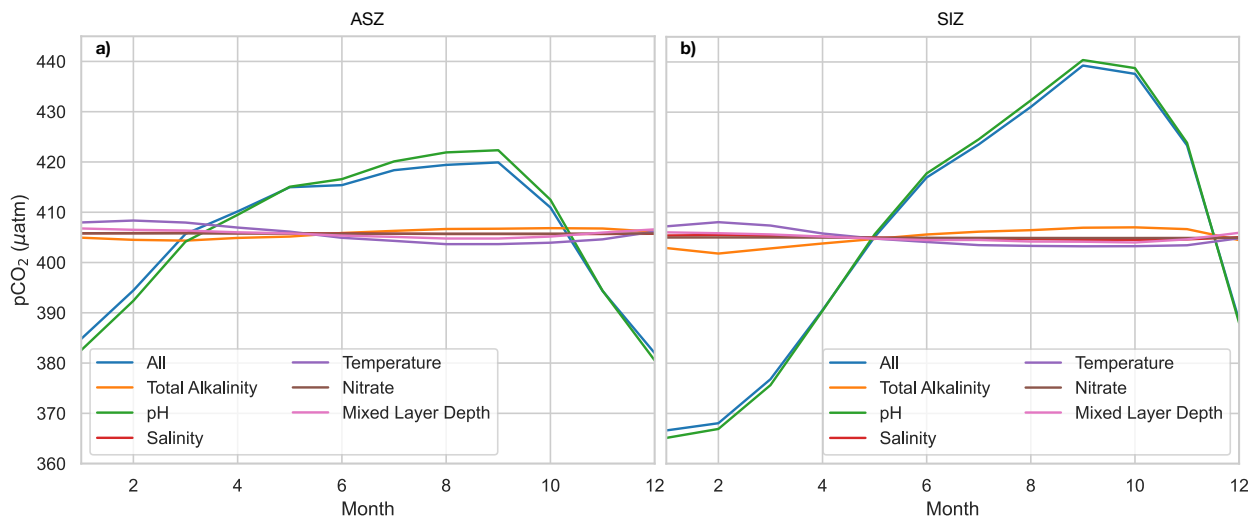
Figure S17. Contribution to seasonal variability from each variable necessary to compute pCO$_2$ using CO2SYS for a) the ASZ and b) the SIZ. (All: we vary all variables, pH: we vary pH and set all other variables to their annual average, etc.)